Nuclear Physics **A465** (1987) 714–732
North-Holland, Amsterdam

DETERMINATION OF THE RATIO $\sigma(\bar{p}n)/\sigma(\bar{p}p)$ FROM $\bar{p}^4$He REACTION DATA

F. BALESTRA, M.P. BUSSA, L. BUSSO, L. FAVA, L. FERRERO, D. PANZIERI, G. PIRAGINO and F. TOSELLO

Istituto di Fisica Generale dell'Università di Torino and INFN-Sezione di Torino, Turin, Italy

G. BENDISCIOLI, A. ROTONDI, P. SALVINI and A. ZENONI

Dipartimento di Fisica Nucleare e Teorica dell'Università di Pavia and INFN-Sezione di Pavia, Pavia, Italy

C. GUARALDO and A. MAGGIORA

Laboratori Nazionali di Frascati dell'INFN, Frascati, Italy

Yu.A. BATUSOV, I.V. FALOMKIN, F. NICHITIU and G.B. PONTECORVO

Joint Institute for Nuclear Research, Dubna, USSR

E. LODI RIZZINI

Dipartimento di Automazione Industriale dell'Università di Brescia and INFN-Sezione di Pavia, Pavia, Italy

Received 4 August 1986
(Revised 8 October 1986)

Abstract: The ratio R_b^a between the cross sections for the annihilation of $\bar{p}$ on n and on p bound in the ^{4}He nucleus at four $\bar{p}$ momenta (at rest, 192.8, 306.2 and 607.7 MeV/c) has been obtained by the analysis of $\bar{p}^4$He annihilation events detected with a self-shunted streamer chamber exposed to the LEAR $\bar{p}$ beams. R_b^a increases from 0.42 ± 0.05 at rest up to 0.66 ± 0.09 at 607.7 MeV/c. The results are discussed in the light of Glauber theory analyses of $\bar{p}^2$H and $\bar{p}$-nucleus data.

E | NUCLEAR REACTION ^{4}He(p-bar, X), $E = 0$, 19.6, 46.7, 179.6 MeV; measured annihilation $\sigma(\bar{p})n/\sigma(\bar{p})p$ for bound nucleons, deduced total $\sigma(\bar{p})n/\sigma(\bar{p})n$ for free nucleons.

1. Introduction

While the interactions of antiprotons with free protons can be studied by using hydrogen targets, the interaction with free neutrons can be studied through the analysis of the $\bar{p}$-nucleus interaction data. Below 600 MeV/c, recently many new results concerning scattering and annihilation of antiprotons on nuclei with $A =$ 4–208 [see refs. [1,2]) and references therein], have been added to the preceding analyses on deuterium [3–7]) so giving new support to the investigation on the $\bar{p}n$ interaction.

0375-9474/87/$03.50 © Elsevier Science Publishers B.V.
(North-Holland Physics Publishing Division)

We consider two different analyses of the $\bar{p}$-nucleus annihilation events which allow to obtain two quantities related to the $\bar{p}n$ and $\bar{p}p$ elementary interactions: (i) the ratio between the cross sections for annihilation on n and on p bound in the nucleus ($R_b^a = \sigma_b^a(\bar{p}n)/\sigma_b^a(\bar{p}p)$) and (ii) the ratio between the total cross sections for the interaction of the antiproton with free n and p ($R_f^T = \sigma(\bar{p}n)/\sigma(\bar{p}p)$).

R_b^a is obtainable in the cases where the annihilation events on n and on p can be recognized through the identification of the products of the reaction, as in the $\bar{p}^2H$ interaction [3,4]). Neglecting charge-exchange effects, in this case $\bar{p}p$ annihilations produces equal numbers of negative and positive pions; in the $\bar{p}n$ annihilations, the number of π^- exceeds by one the number of π^+ and a recoil proton is present.

R_f^T is obtainable from $\bar{p}$-nucleus scattering data through a Glauber theory analysis. Indeed, due to the high annihilation probability and the consequent diffractive character of the elastic scattering, the Glauber theory has been shown to be suitable for describing the low-energy $\bar{p}$-nucleus interaction [1,6,8]). Therefore, if one assumes that the $\bar{p}p$ interaction parameters and the nuclear matter distribution are known, this approach allows one to calculate the total cross section for the interaction of antiprotons with free neutrons and the ratio R_f^T.

Schematically, our present knowledge on R_b^a and R_f^T is as follows. Concerning the $\bar{p}^2H$ interaction, first the values of R_b^a are known for antiproton momenta above 260 MeV/c from ref. [4]) and above 300 MeV/c from ref. [3]). The two sets of values agree well and indicate that $R_b^a < 1$ (increasing with the momentum). Second, Glauber theory analyses of deuterium data between 300 and 600 MeV/c led to different sets of R_f^T values versus $\bar{p}$ momentum in relation to different sets of experimental total cross section values. Specifically, the data from refs. [3,4]) lead to $R_f^T > 1$ (increasing as the momentum decreases; see refs. [7,9]) and those from ref. [10]) lead to $R_f^T < 1$ (increasing with the momentum; see ref. [9])). One finds that the values of $R_f^T < 1$ and of R_b^a agree well within the experimental errors.

Concerning $\bar{p}$-nucleus data [1,2,11]), the results of some Glauber theory analyses with $A > 4$ above 300 MeV/c agree with $R_f^T < 1$, refs. [1,8,9,12]).

Our aim is to contribute to this field by performing a measurement of the R_b^a and R_f^T ratios in the $\bar{p}^4$He interaction from respectively the annihilation events and a Glauber theory analysis of the reaction cross sections at 200, 300, 600 MeV/c [ref. [13])] and at rest. The data taken at rest are presented here for the first time. The data were obtained with a streamer chamber in a magnetic field exposed to the LEAR antiproton beams [14,15]).

The work is organized as follows. In sect. 2 and sect. 3 the procedure to extract $\sigma^a(\bar{p}n)$, $\sigma^a(\bar{p}p)$ and R_b^a from recognized events is explained. In sect. 4 this procedure is applied to the data at rest, at 200, 300 and 600 MeV/c. In sect. 5 Glauber theory calculations of R_f^T are performed. Finally, in sect. 6 our results are discussed and compared with those of other authors. Our main results can be summarized as follows. The R_b^a values are 0.42 ± 0.05 at rest, 0.64 ± 0.07 at 192.8 MeV/c, 0.69 ± 0.06 at 306.2 MeV/c, and 0.66 ± 0.09 at 607.7 MeV/c; i.e., R_b^a for the $\bar{p}^4$He interaction

increases with the $\bar{p}$ momentum as in the $\bar{p}^2$H interaction [3,4]). However, the ^{4}He values are somewhat smaller than the ^{2}H ones particularly at 600 MeV/c. Moreover, our results at 200 and 300 MeV/c, the previous $\bar{p}^2$H annihilation data and some data from Glauber theory analyses of $\bar{p}^2$H and $\bar{p}$-nucleus total cross sections [this work and refs. [1,8,9,12])] show an overall agreement within the experimental uncertainties on the condition

$$R_b^a \approx R_f^T < 1$$

with R increasing with $\bar{p}$ momentum.

2. $\bar{p}^4$He annihilation

2.1. INTRODUCTION

The $\bar{p}^4$He annihilation process may consist of the following reaction sequence:

(a) inelastic scattering (charge exchange, knock-out, break-up); we will call it initial state interaction (ISI);

(b) antinucleon-nucleon annihilation;

(c) interaction between the residual nucleons and the annihilation mesons (mostly pions); we will call it final state interaction (FSI).

If only annihilation is effective and ISI and FSI are not, $\bar{p}p$ annihilation produces an odd number of charged prongs (1 heavy prong, i.e. a ^{3}H nucleus, and an even number of charged pions) and $\bar{p}n$ annihilation produces an even number of charged prongs (1 heavy prong, i.e. a ^{3}He nucleus, and an odd number of charged pions). Hence, the two types of annihilation processes are distinguishable by the numbers of charged prongs.

2.2. ISI EFFECTS ON THE NUMBER OF THE CHARGED PRONGS

Let us consider the occurrence of the reactions (a) and (b). In this case a number of different processes may occur, such as those sketched in fig. 1.

The knock-out and break-up processes may prevent the presence of ^{3}H and ^{3}He among the final products of the annihilation processes, so favouring the increase of the number of events with an odd number of prongs in respect of that of the even prong ones. Nevertheless, $\bar{p}p$ and $\bar{p}n$ annihilation events are in principle still distinguishable. Indeed, the $\bar{p}p$ annihilation events have among the final products one heavy prong and a number of negative pions equal to that of the positive pions. Instead, the $\bar{p}n$ annihilation events produce odd prong events with two heavy prongs and a number of negative pions greater than that of the positive pions (+1).

The charge exchange process changes $\bar{p}$ into $\bar{n}$; due to the isospin states, the $\bar{n}n$ annihilation is identical to the $\bar{p}p$ one (i.e. they have the same cross section) and the $\bar{n}p$ process is equal to the $\bar{p}n$ one.

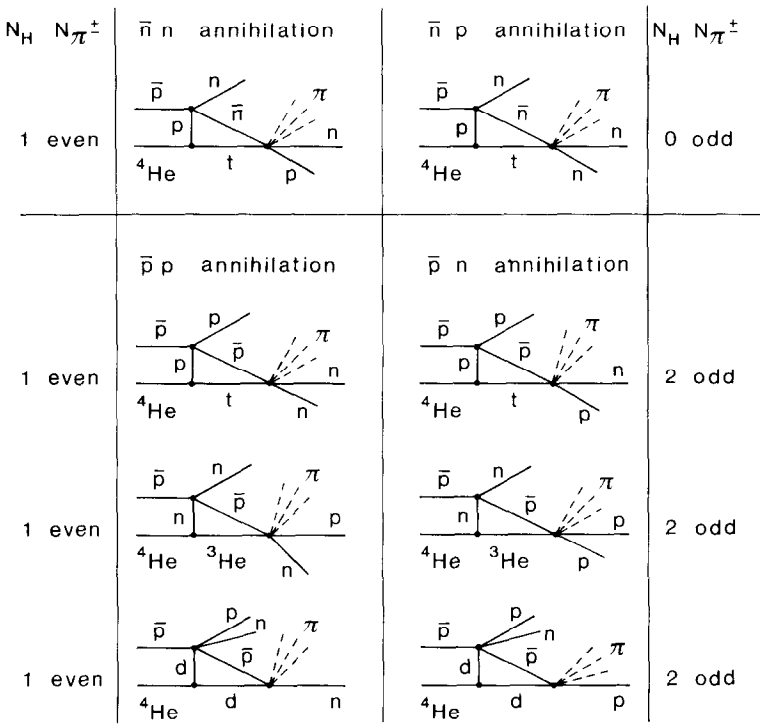

Fig. 1. Different reaction schemes of annihilation preceded by ISI. N_H = number of heavy prongs after the processes (a) and (b). $N_{\pi^\pm}$ = Number of charged pions.

The occurrence of charge exchange could have the main consequence that the R_a^b ratio for bound nucleons is lower than the like ratio for free nucleons, because the produced n̄ may interact further with two neutrons and one proton, so that the n̄n annihilation is favoured statistically 2 : 1 in respect of the n̄p one. We can estimate the depression of R_a^b as follows. If we indicate with R' the undepressed quantity, we have $R \approx aR' + \frac{1}{2}bR'$, where a is the percentage of annihilation events without charge exchange and b is the percentage with charge exchange. Assuming for b the values for free protons (3.6%, 6.5% and 7% at 200, 300 and 600 MeV/c, respectively; see refs. [16-20])), we obtain $(R'-R)/R' = 1.8\%$, 3.2% and 3.8%, respectively.

2.3. FSI EFFECTS ON THE NUMBER OF THE CHARGED PRONGS

Now let us consider annihilations followed by FSI, neglecting ISI. FSI may break the ^{3}He and ^{3}H nuclei increasing the number of events with an odd total number of charged prongs; moreover it may change the primary numbers of heavy prongs and charged pions through the pion-nucleon charge exchange interaction. The possible reactions are listed in table 1. An important consequence of the charge exchange, due to the $\pi^- p \to \pi^0 n$ and $\pi^0 p \to \pi^+ n$ reactions, is that the p̄p annihilation

events assume the features of events due to $\bar{p}n$ annihilation and vice versa, as it concerns the relative numbers of heavy and light particles emitted. For instance, reaction (A) in table 1 may be due to a direct $\bar{p}p$ annihilation or to a $\bar{p}n$ annihilation followed by the $\pi^- p \to \pi^0 n$ reaction; reaction (B) may be due to a direct $\bar{p}n$ annihilation or to a $\bar{p}p$ annihilation followed by the $\pi^+ n \to \pi^0 p$ reaction. Therefore, the distinction between events due to $\bar{p}n$ and $\bar{p}p$ annihilation is not possible, in general, on the basis of the numbers of heavy and light particles.

However, one has to notice that πN charge exchange is less probable than πN scattering as the respective cross sections are approximately in the ratio

$$\sigma(\pi^+ p) : \sigma(\pi^0 p) : \sigma(\pi^- p) : \sigma_{ce} = 9 : 4 : 1 : 2$$

the annihilation pion momenta being close to the baryonic resonance momentum ($\sim$300 MeV/c).

2.4. CONCLUSIONS

The same conclusions hold also for the case where ISI is taken into account. The possible final state configurations are the same as reported in table 1. Processes including $\bar{n}n$ annihilation develop as those including $\bar{p}p$ annihilation.

Therefore we summarize the above analysis as follows:

(i) $\bar{p}^4$He annihilation events may have an even or an odd number of charged prongs.

(ii) Even prong events are due to $\bar{p}n$ annihilation only; among their final products there are 1 heavy prong (^{3}He) and an odd number of charged pions.

(iii) Odd prong events arise both from direct $\bar{p}p$ annihilation and from $\bar{p}p$ or $\bar{p}n$ annihilation followed by FSI or preceded by ISI.

(iv) Due to final πN charge exchange, $\bar{p}p$ and $\bar{p}n$ annihilation events with an odd total number of charged prongs are in general not distinguishable.

In spite of point (iv), it is possible to extract information from the odd prong events which allows us to evaluate the ratio between the cross sections for the $\bar{p}n$ and $\bar{p}p$ annihilations, as we will show in the next section.

3. $\bar{p}n$ and $\bar{p}p$ annihilation cross sections

3.1. ODD PRONG EVENTS ANALYSIS

Odd prong events may be shared into two sets (a) and (b): (a) includes (i) direct $\bar{p}p$ annihilations; (ii) $\bar{p}p$ annihilations plus FSI without final charge exchange on n (π^0n, π^+n); (iii) $\bar{p}n$ annihilations plus final charge exchange on p (π^0p, π^-p). Set (a) includes mostly $\bar{p}p$ annihilations and $\bar{p}n$ annihilations which look like $\bar{p}p$ annihilations owing to pion charge exchange.

TABLE 1

Examples of reactions due to annihilation plus FSI as the number of annihilation $\pi^{\pm}$ increases from 0 to 3

$\bar{p}^4$He annihilation type	FSI effect	set	reaction type	N_T	N_H	$E^{\pm}$
$(\bar{p}p)^* \to t + M\pi^0 \to p + 2n + M\pi^0$		a	A	1	1	=
	$[\pi^0 n \to \pi^- p] \to 2p + n + \pi^- + M\pi^0$	b	B	3	2	$\neq$
	$[\pi^0 p \to \pi^+ n] \to 3n + \pi^+ + M\pi^0$	a	C	1	0	$\neq$
$(\bar{p}n)^* \to {}^3He + \pi^- + M\pi^0 \to 2p + n + \pi^- + M\pi^0$		b	B	3	2	$\neq$
	$[\pi^0 p \to \pi^+ n] \to p + 2n + \pi^- + \pi^+ + M\pi^0$	a	D	3	1	=
	$[\pi^- p \to \pi^0 n] \to p + 2n + M\pi^0$	a	A	1	1	=
	$[\pi^0 n \to \pi^- p] \to 3p + 2\pi^- + M\pi^0$	b	E	5	3	$\neq$
$(\bar{p}p)^* \to t + \pi^- + \pi^+ + M\pi^0 \to p + 2n + \pi^- + \pi^+ + M\pi^0$		a	D	3	1	=
	$[\pi^0 n \to \pi^- p] \to 2p + n + 2\pi^- + \pi^+ + M\pi^0$	b	F	5	2	$\neq$
	$[\pi^0 p \to \pi^+ n] \to 3n + \pi^- + 2\pi^+ + M\pi^0$	a	G	3	0	$\neq$
	$[\pi^- p \to \pi^0 n] \to 3n + \pi^+ + M\pi^0$	a	C	1	0	$\neq$
	$[\pi^+ n \to \pi^0 p] \to 2p + n + \pi^- + M\pi^0$	b	B	3	2	$\neq$
$(\bar{p}n)^* \to {}^3He + 2\pi^- + \pi^+ + M\pi^0 \to 2p + n + 2\pi^- + \pi^+ + M\pi^0$		b	I	5	2	$\neq$
	$[\pi^- p \to \pi^0 n] \to p + 2n + \pi^- + \pi^+ + M\pi^0$	a	G	3	1	=
	$[\pi^0 n \to \pi^- p] \to 3p + 3\pi^- + \pi^+ + M\pi^0$	b	L	7	3	$\neq$
	$[\pi^0 p \to \pi^+ n] \to p + 2n + 2\pi^- + 2\pi^+ + M\pi^0$	a	N	5	1	=
	$[\pi^+ n \to \pi^0 p] \to 3p + 2\pi^- + M\pi^0$	b	F	5	3	$\neq$

πN scattering and charge exchange effects are shown separately. In square parentheses the different charge exchange reactions are indicated. Deuterons are omitted among the final products for the sake of simplicity. a, b, etc. indicate reactions with different types of charged particles in the final state. N_T is the total number of charged particles, N_H is the number of heavy particles and $E^{\pm}$ is the equality (=) or the inequality ($\neq$) of the numbers of charged pions.

(b) includes (i) $\bar{p}n$ annihilations plus FSI without final charge exchange on p ($\pi^0 p$, $\pi^- p$); (ii) $\bar{p}p$ annihilations plus final charge exchange on n ($\pi^+ n$, $\pi^0 n$).

Set (b) includes mostly $\bar{p}n$ annihilations and $\bar{p}p$ annihilations which look like $\bar{p}n$ annihilations owing to pion charge exchange.

The events belonging to the two sets can be recognized through the numbers of heavy prongs and the equality between the numbers of π^+ and π^-, as it is summarized in table 2. Of course, all the events with one prong belong to the set (a), while the events with a higher multiplicity may belong both to the set (a) and to the set (b).

3.2. EVALUATION OF $\sigma^a(\bar{p}n)$, $\sigma^a(\bar{p}p)$ AND R_b^a

We define: $\sigma_m(\bar{p}p)$ = cross section for (a) event production; $\sigma_m(\bar{p}n)$ = cross section for (b) event production; $\sigma^a(\bar{p}p)$ = cross section for annihilation on p; $\sigma^a(\bar{p}n)$ = cross section for annihilation on n; $\sigma_{ce}^p(\bar{p}n)$ = cross section for annihilation on n plus final charge exchange on p; $\sigma_{ce}^n(\bar{p}p)$ = cross section for annihilation on p plus final charge exchange on n; σ_e^a = cross section for even prong event production (^{3}He production); σ_0^a = cross section for odd prong event production. σ_e^a and σ_0^a are known from

TABLE 2

Features of the charged prongs of the events of type (a) and (b) (see text)

	N_H	$E^{\pm}$
(a) events	0	$\neq$
	1	$=$
(b) events	≥ 2	$\neq$

N_H = number of heavy prongs; $E^{\pm}$ = equality ($=$) or inequality ($\neq$) of the numbers of π^- and π^+.

published data [13]). $\sigma_m(\bar{p}p)$ and $\sigma_m(\bar{p}n)$ are measured in the present analysis. $\sigma^p_{ce}(\bar{p}n)$ and $\sigma^n_{ce}(\bar{p}p)$ are unknown and should be obtained from the event analysis, which is not easy. However their contribution is negligible (see later on). $\sigma^a(\bar{p}p)$ and $\sigma^a(\bar{p}n)$ are annihilation cross sections on nucleons bound in ^{4}He and include the direct $\bar{p}$-nucleon annihilation cross sections and all the interference terms due ISI and FSI; $\sigma^p_{ce}(\bar{p}n)$ and $\sigma^n_{ce}(\bar{p}p)$ have a like meaning.

By definition, the following relations hold:

$$\sigma^a(\bar{p}p) = \sigma_m(\bar{p}p) - \sigma^p_{ce}(\bar{p}n) + \sigma^n_{ce}(\bar{p}p) = \sigma_m(\bar{p}p) - \sigma_{ce}\,, \tag{3.1}$$

$$\sigma^a(\bar{p}n) = \sigma_m(\bar{p}n) + \sigma^a_e + \sigma^p_{ce}(\bar{p}n) - \sigma^n_{ce}(\bar{p}p) = \sigma_m(\bar{p}n) + \sigma^a_e + \sigma_{ce}\,, \tag{3.2}$$

$$\sigma^a(\bar{p}p) + \sigma^a(\bar{p}n) = \sigma^a_e + \sigma^a_0\,, \tag{3.3}$$

where

$$\sigma_{ce} = \sigma^p_{ce}(\bar{p}n) - \sigma^n_{ce}(\bar{p}p) \tag{3.4}$$

contains terms which tend to cancel each other ($\pi^0 p \rightleftarrows \pi^+ n$; etc.) [3]).

Having set

$$r = \frac{\sigma_m(\bar{p}n)}{\sigma_m(\bar{p}p)} \tag{3.5}$$

from eqs. (3.1), (3.2) and (3.3) one obtains

$$\sigma^a(\bar{p}p) = \sigma^a_0 \frac{1-(1+r)\sigma_{ce}/\sigma^a_0}{1+r}\,, \tag{3.6}$$

$$\sigma^a(\bar{p}n) = \sigma^a_0 \frac{(1+r)\sigma^a_e/\sigma^a_0 + r + (1+r)\sigma_{ce}/\sigma^a_0}{1+r}\,, \tag{3.7}$$

$$R^a_b = \frac{\sigma^a(\bar{p}n)}{\sigma^a(\bar{p}p)} = \frac{(1+r)\sigma^a_e/\sigma^a_0 + r + (1+r)\sigma_{ce}/\sigma^a_0}{1-(1+r)\sigma_{ce}/\sigma^a_0}\,. \tag{3.8}$$

By assuming

$$\sigma_{cc}/\sigma_0^a \ll 1 \tag{3.9}$$

one obtains the simplified formulas:

$$\sigma^a(\bar{p}p) \simeq \frac{\sigma_0^a}{1+r}, \tag{3.10}$$

$$\sigma^a(\bar{p}n) \simeq \sigma_e^a + \frac{r}{1+r}\sigma_0^a, \tag{3.11}$$

$$R_b^a = \frac{\sigma^a(\bar{p}n)}{\sigma^a(\bar{p}p)} \simeq (1+r)\frac{\sigma_e^a}{\sigma_0^a} + r. \tag{3.12}$$

4. Experimental data analysis

4.1. DATA AT 19.6 MeV AND AT REST

We have measured non-elastic events at 19.6 MeV (198.8 MeV/c), an energy where inelastic processes are forbidden and only annihilation is possible. Cross sections and charged prong multiplicity distributions are given in ref. [13]) and the data useful in the present work are reported in the tables 3 and 4b. We recall that the production of ^{3}He is evidentiated simply by an even number of charged prongs.

TABLE 3

Annihilation cross sections

E (MeV)	at rest	19.6	48.7	179.6
σ_e^a	(21.26 ± 1.15)%	93.2 ± 7.9	58.6 ± 4.1	33.0 ± 1.7
σ_0^a	(78.73 ± 2.21)%	312.4 ± 14.3	229.0 ± 8.1	196.9 ± 4.2
σ_t^a		405.6 ± 16.4	287.6 ± 9.1	229.9 ± 4.6
σ_e^a/σ_0^a	0.270 ± 0.016	0.298 ± 0.029	0.255 ± 0.021	0.167 ± 0.0096

(t) total, (e) even prong event production, (o) odd prong event production (values from ref. [13]) minus charge exchange cross sections); the cross section values are in mb for annihilation in flight and % at rest.

Also we have performed measurements of momenta and angles and mass identification to which we will refer in detail elsewhere [14]). Here we limit ourselves to say that we were able to recognize the mass of the particles (or, at least, to distinguish between pions and heavy particles) in 72% of the tracks on the basis of the following information: (i) the geometrical characteristics of the tracks given by the Hydra geometry program for different mass hypotheses; (ii) the relative ionizations of the tracks on the same picture; (iii) the electric charge conservation and (iv) the barionic number conservation. This information allowed us to identify 286 events with 3, 5 and 7 prongs as belonging to the set (a) or to the set (b). We recall that all the one

prong events belong to the set (a) and are the 4.7% of the odd prong events (see table 4b).

Mass identification is prevented mainly in the cases of tracks at small angles in respect of the magnetic field direction or with very low ionization (very fast particles). These limitations might introduce a systematic error into the ratio r between the numbers of events of type (b) and type (a).

TABLE 4

Observed events of type (a) and type (b) and related multiplicity distributions at four $\bar{p}$ energies

(a)

at rest									
1		2			3	4	5	6	7
n_c	n_{π^-}	N_{ev} (a)	(b)	(a)+(b)	P_i	% (a)	% (b)	% $\bar{p}p$	% $\bar{p}n$
1	0				3.9±0.5	3.9±0.5		3.9±0.5	
2	1				6.8±0.6				8.9±1.3
3	1	43	3	46	34.9±1.5	32.9±1.8	2.0±1.1	32.9±1.8	
4	2				11.3±0.8				16.04±2.0
5	2	30	5	35	34.1±1.5	29.0±2.2	5.1±1.8	29.0±2.2	
6	3				3.1±0.4				4.4±1.2
7	3	2	1	3	5.5±0.6	4.1±1.3	1.4±1.2	4.1±1.3	
8	4				0.06±0.06				0.06±0.06
9	4				0.19±0.11			0.19±0.11	
$\langle n_{\pi^-} \rangle$								1.48±0.07	1.84±0.19

(b)

192.8 MeV/c (19.6 MeV)									
1		2			3	4	5	6	7
n_c	n_{π^-}	N_{ev} (a)	(b)	(a)+(b)	P_i	% (a)	% (b)	% $\bar{p}p$	% $\bar{p}n$
1	0				4.7±0.9	4.7±0.9		4.7±0.9	
2	1				6.7±1.0				8.4±1.2
3	1	121	7	128	31.0±2.2	29.3±2.1	1.7±0.6	29.3±2.1	
4	2				13.1±1.5				24.7±2.2
5	2	93	43	136	36.6±2.4	25.0±2.1	11.6±1.6	25.0±2.1	
6	3				2.9±0.7				5.5±0.8
7	3	9	13	22	4.4±0.8	1.8±0.5	2.6±0.5	1.8±0.5	
8	4				0.16±0.16				0.16±0.16
9	4				0.16±0.16			0.16±0.16	
$\langle n_{\pi^-} \rangle$								1.40±0.08	1.93±0.10

TABLE 4—continued

(c)

306.2 MeV/c (47.9 MeV)									
1		2			3	4	5	6	7
n_c	n_{π^-}	N_{ev} (a)	(b)	(a)+(b)	P_i	% (a)	% (b)	% $\bar{p}p$	% $\bar{p}n$
1	0				3.3 ± 0.4	3.3 ± 0.4		3.3 ± 0.4	
2	0, 1				5.3 ± 0.7				6.7 ± 1.6
3	0, 1	45	2	47	32.9 ± 1.8	31.5 ± 2.0	1.4 ± 1.0	31.2 ± 2.0	
4	2				11.1 ± 1.0				24.1 ± 2.7
5	2	32	18	50	36.0 ± 1.9	23.0 ± 2.7	13.0 ± 2.5	23.0 ± 2.7	
6	3				3.7 ± 0.6				9.8 ± 1.4
7	3	1	5	6	7.3 ± 0.8	1.2 ± 1.1	6.1 ± 1.3	1.2 ± 1.1	
8	4				0.19 ± 0.14				0.19 ± 0.14
9	4				0.10 ± 0.10			0.10 ± 0.10	
$\langle n_{\pi^-} \rangle$								1.38 ± 0.11	2.08 ± 0.17

(d)

607.7 MeV/c (199.6 MeV)									
1		2			3	4	5	6	7
n_c	n_{π^-}	N_{ev} (a)	(b)	(a)+(b)	P_i	% (a)	% (b)	% $\bar{p}p$	% $\bar{p}n$
1	0				5.2 ± 0.6	5.2 ± 0.6		5.2 ± 0.6	
2	0, 1				4.0 ± 0.4				10.1 ± 2.0
3	0, 1	35	8	43	32.7 ± 0.1	26.6 ± 2.2	6.1 ± 1.9	26.6 ± 2.0	
4	2				7.5 ± 0.6				22.8 ± 3.1
5	2	24	15	39	39.6 ± 1.3	24.4 ± 3.2	15.2 ± 3.1	24.4 ± 3.2	
6	3				2.6 ± 0.3				6.6 ± 1.9
7	3	2	2	4	7.9 ± 0.6	4.0 ± 2.0	4.0 ± 2.0	4.0 ± 2.0	
8	4				0.13 ± 0.08				0.24 ± 0.14
9	4	-	1	1	0.11 ± 0.11		0.11 ± 0.11		
$\langle n_{\pi^-} \rangle$								1.46 ± 0.14	1.92 ± 0.22

n_c = charged prong multiplicity; n_{π^-} = negative pion multiplicity; N_{ev} = number of events of type (a) or (b) and (a) + (b); P_i = charged prong multiplicity distributions from ref. [13]), charge exchange contributions having been subtracted (we notice that the multiplicity distribution at 600 MeV/c refers to a two time higher statistics than in ref. [13]); % (a) = normalized percentages of events of type (a); % (b) = as above for the type (b) ones; % ($\bar{p}p$) = multiplicity distribution for $\bar{p}p$ annihilations (from column 4); % ($\bar{p}n$) = multiplicity distribution for $\bar{p}n$ annihilations (from columns 3 and 5 of table 4b: 8.4 = 6.7 + 1.7, etc).

However, we notice that the relative percentages of the recognized events with 3, 5 and 7 prongs are equal, within statistical error, to the corresponding percentages for all the events (44.8 ± 3.8, 47.7 ± 4.1, 7.8 ± 1.6 to be compared to 43.0 ± 3.1, 50.8 ± 3.3 and 6.1 ± 1.1, respectively) and the mean numbers of negative pions associated to the (a) type events and to the (b) type ones plus the even prong ones are equal, respectively, to the values expected for $\bar{p}p$ and $\bar{p}n$ annihilations (1.38 ± 0.10 and 1.95 ± 0.12 to be compared to 1.49 ± 0.02 and 2.08 ± 0.04, respectively [3,4,16,17]). Hence we conclude that possible systematic errors in the identification of the two types of events are within the statistical errors.

In order to evaluate the quantities defined by formulas (3.6)-(3.8) or (3.10)-(3.12), we calculated the ratio σ_{ce}/σ_0^a in an approximate way as follows. In the $\bar{p}p$ annihilation the residual nucleons are (p+2n) and, on the average, the number of the produced pions is $(1.5\pi^+ + 1.5\pi^- + 2\pi^0)$. In the $\bar{p}n$ annihilation the residual nucleons are (n+2p) and the pions are $(1\pi^+ + 2\pi^- + 2\pi^0)$ [refs. [3,4,16,17])]. Considering the possible π-nucleon pairs and the ratios between the corresponding cross sections (see sect. 2.3), one obtains

$$\sigma_{ce}^{n}(\bar{p}p)/\sigma_{FSI}(\bar{p}p) \approx 0.15\,,$$

$$\sigma_{ce}^{p}(\bar{p}n)/\sigma_{FSI}(\bar{p}n) \approx 0.18\,,$$

where $\sigma_{FSI}(\bar{p}p)$ indicates the total cross section for the interaction of the pions and the residual nucleons after the $\bar{p}p$ annihilation; a similar meaning holds for $\sigma_{FSI}(\bar{p}n)$. Assuming [1,6,8,9]) $\sigma^a(\bar{p}n)/\sigma^a(\bar{p}p) = 0.7$-1 and considering that FSI occurs in at most 44% of the annihilation events [13]), the values of σ_{ce}/σ_0^a are between -0.009 and 0.017, that is

$$\frac{\sigma_{ce}}{\sigma_0^a} \ll 1\,.$$

Hence, we assume that the simplified formulas (3.10)-(3.12) may be used.

For the effective evaluation of r, we calculated for each multiplicity i the fractions of the (0, 1) heavy prong events and of the (≥ 2) heavy prong events (the numbers of the events are given in column 2 of table 4b) and multiplied them by the multiplicity percentage P_i (column 3), so obtaining the values reported in the column 4 and 5 of the same table. In this way we normalized the fractions of the events of column 2 to the multiplicity percentages concerning all the measured events, so compensating for possible systematic errors made in the identification of the events of type (a) or (b).

The results are given in table 5 and fig. 2.

A similar procedure was applied to a sample of at-rest events. The measured quantities are given in tables 3 and 4a and the calculated quantities are reported in table 5 and fig. 2.

4.2. DATA AT 48.7 AND 179.6 MeV

These energies are higher than the energy threshold for charge exchange ($\bar{p}p \to \bar{n}n$) and for break-up and knock-out reactions. The charge exchange (not followed by annihilation) contributes to one prong events only and the other processes contribute to 2 and 3 charged prong events [13]).

Between 300 and 600 MeV/c the charge exchange cross section is 10–12% of the annihilation cross section on free protons [18,22]); in deuterium the same percentage is 1.5–2% [ref. [3])]; in carbon at 600 MeV/c it is 2.2% [ref. [23])]. We assumed the last value to hold also for ^{4}He at 300 and 600 MeV/c and corrected consequently the cross-section values reported in ref. [13]). The corrected values are reported in table 3. In tables 4c, d the corrected charged prong multiplicity distributions are listed.

No correction has been introduced to eliminate possible break-up and knock-out events which were estimated as less than 3% of all non-elastic events [13]).

We analyzed the 300 and 600 MeV/c events with the same procedure followed for those at 200 MeV/c. All data are reported in table 4c, d and their quality is like that of the 200 MeV/c data. The values of r, R_b^a, $\sigma^a(\bar{p}p)$ and $\sigma^a(\bar{p}n)$ are shown in table 5, figs. 2 and 3.

TABLE 5

Cross sections for annihilation on p and on n and their ratios (see text); the cross-section values are in mb for annihilation in flight and % at rest

MeV/c MeV	at rest	192.8 19.6	306.2 48.7	607.7 179.6
r	0.12 ± 0.04	0.26 ± 0.05	0.35 ± 0.04	0.42 ± 0.07
$R_b^a = \frac{\sigma^a(\bar{p}n)}{\sigma^a(\bar{p}p)}$	0.42 ± 0.05	0.64 ± 0.07	0.69 ± 0.06	0.66 ± 0.09
$\sigma^a(\bar{p}p)$	(70.4 ± 2.5)%	247.8 ± 14.6	170.1 ± 8.2	138.5 ± 7.8
$\sigma^a(\bar{p}n)$	(29.6 ± 2.5)%	157.8 ± 21.9	117.5 ± 12.2	91.5 ± 9.1

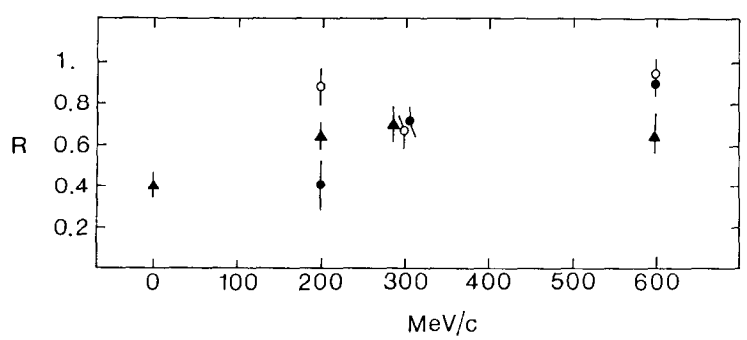

Fig. 2. (▲) R_b^a values obtained in sect. 4; (○) R_f^T values calculated by means of the Glauber theory with the $\bar{p}p$ data of ref. [32]); (●) R_f^T values calculated with the $\bar{p}p$ data of ref. [31]).

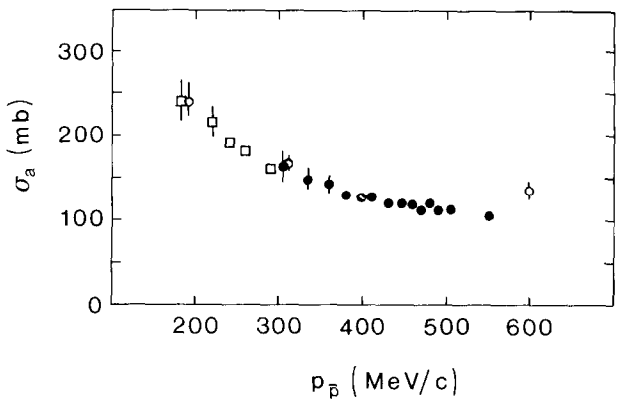

Fig. 3. $\bar{p}p$ annihilation cross section: (●) ref. [20]), (□) ref. [31]); cross section for annihilation of $\bar{p}$ on p bound in ^{4}He: (○).

In fig. 3 the $\sigma^a(\bar{p}p)$ values are compared with the values of $\sigma^a(\bar{p}p)$ for free protons. One sees that $\sigma^a(\bar{p}p) \approx \sigma_f^a(\bar{p}p)$, so that the cross section per proton for $\bar{p}$ annihilation on p bound in ^{4}He is only $\frac{1}{2}\sigma_f^a$. Evidently, the compact structure of ^{4}He produces a strong shadow effect, a situation quite different from the annihilation on ^{2}H, where, due to the soft structure, one finds $\sigma^a(\bar{p}p) = \sigma^a(\bar{p}p)$ [refs. [5,6])].

5. Glauber theory calculation of R_f^T

As is known, the Glauber approximation of hadron-nucleus scattering is based on the projectile-free nucleon amplitudes and neglects off-shell and rescattering (i.e. multiple scattering on the same nucleon) effects.

The limits of validity of this approach have been a long standing problem of nuclear reaction theory [24]). Now it is definitely established that, when the eikonal propagator is employed in the Watson multiple scattering expansion of the on-shell transition amplitude, for commuting interactions there is a complete cancellation between off-shell and rescattering effects, and one obtains the Glauber multiple scattering series [25]). This means that the off-shell effects are present only on the longitudinal part of the transferred momentum and they are negligible when the diffractive nature of the interaction permits the use of the eikonal (Glauber) approximation.

Since the $\bar{p}$-nucleon interaction is commutative when spin effects are neglected and is diffractive even at low energy, one concludes that the Glauber approximation is applicable (and in effect it has been successfully applied [1,6,8,12])), in the analysis of low-energy $\bar{p}$-nucleus scattering.

From the above discussion it results also that the relative accuracy of this approximation in calculating total cross sections is given by the weight of the noneikonal effects on the eikonal ones in the Watson multiple scattering expansion

of the transition amplitude [24,25]). This weight amounts [6,26]) to $(kR_0)^{-1}\,\mathrm{Re}\,f(0)/\mathrm{Im}\,f(0)$, where $f(0)$ is the $\bar{p}$-nucleon scattering amplitude at 0°, k is the projectile momentum and R_0 the nuclear radius. Since in the low-energy $\bar{p}p$ scattering $\mathrm{Re}\,f(0)/\mathrm{Im}\,f(0) \leqslant 0.2$ for $200 < k < 600\ \mathrm{MeV}/c$, we estimated that the inaccuracy of our Glauber approach in what follows is <5% (from table 6).

We define, as usually, the $\bar{p}$-free nucleon scattering amplitude in the form

$$f(q) = (k/4\pi)\sigma_j(i+\rho_j)\,\mathrm{e}^{-\beta_j^2 q^2/2}\,, \tag{5.1}$$

where q is the transferred momentum, $\rho_j = \mathrm{Re}\,f(0)/\mathrm{Im}\,f(0)$, β_j^2 is the slope parameter and σ_j the $\bar{p}$-nucleon total cross section. The index j defines the target nucleon ($j = \mathrm{p}$ and $j = \mathrm{n}$ for protons and neutrons, respectively). With these definitions, the $\bar{p}^4$He scattering amplitude in the Glauber approximation is [27,28])

$$F(\Delta) = ik\,\mathrm{e}^{R_0^2\Delta^2/16}\int J_0(\Delta b)\{1-(1-(1-i\rho_\mathrm{p})G_\mathrm{p}(b))^2(1-(1-i\rho_\mathrm{n})G_\mathrm{n}(b))^2\}b\,\mathrm{d}b\,, \tag{5.2}$$

where Δ and Δ^2 are the laboratory transferred 3-momentum and 4-momentum, respectively; J_0 is the Bessel function and

$$G_j(b) = (\sigma_j/8\pi\gamma^2)\,\mathrm{e}^{-b_j^2/4\gamma^2}$$

$$\gamma_j = \tfrac{1}{2}\beta_j^2 + \tfrac{1}{4}R_0^2$$

$$j = \mathrm{n}, \mathrm{p}\,.$$

In eq. (5.2) one assumes for ^{4}He an independent particle model with point-like nuclear densities given by harmonic oscillator wave functions [29]).

In this treatment Pauli, spin and nucleon-nucleon correlations are neglected. However, the first effect is absent from ^{4}He because of the charge and spin variables of the four nucleons. The remaining ones affect the large angle behaviour of the

TABLE 6

Determination of ratio $R_\mathrm{f}^\mathrm{T} = \sigma_\mathrm{n}/\sigma_\mathrm{p} = \beta_\mathrm{n}^2/\beta_\mathrm{p}^2$ using Glauber theory and $\bar{p}p$ scattering amplitude parameters interpolated from refs. [31,32])

			Ref. [32])			Ref. [31])		
Momemtum (MeV/c)	$\sigma_\mathrm{R}^\mathrm{exp}$ (mb)	ρ_p	σ_p (mb)	β_p^2 (GeV^{-2})	R_f^T	σ_p (mb)	β_p^2 (GeV^{-2})	R_f^T
200	406 ± 16	0.05	328	44	0.88 ± 0.09	309	71	0.40 ± 0.12
300	294 ± 9	−0.13	240	32	0.67 ± 0.08	225	32	0.71 ± 0.07
600	235 ± 5	0.20	150	21	0.90 ± 0.06	143	21	0.94 ± 0.06

$\sigma_\mathrm{R}^\mathrm{exp} = \bar{p}^4$He total reaction cross section [13]); $\rho_\mathrm{p} = \mathrm{Re}\,f(0)/\mathrm{Im}\,(0)$ for $\bar{p}p$ interaction, see eq. (5.9); σ_p = total $\bar{p}p$ cross section; β_p^2 = slope parameter of the $\bar{p}p$ amplitude, see eq. (5.1); $\mathrm{R}_\mathrm{f}^\mathrm{T}$ = total $\bar{p}n$ cross section over total $\bar{p}p$ cross section.

elastic scattering distribution by a few percent [30]), so that they have a negligible influence on total cross-section calculations.

The input parameters of the model are R_0, σ_p, β_p^2, ρ_p, σ_n, β_n^2, ρ_n. We fix for ^{4}He $R_0 = 1.37$ fm [refs. [29,30])] and take σ_p, β_p^2, and ρ_p from low-energy $\bar{p}p$ scattering experiments [31,32]). Recalling that we have defined (sect. 1)

$$R_f^T = \sigma(\bar{p}n)/\sigma(\bar{p}p) \tag{5.3}$$

following refs. [6,9]), we assume also

$$\beta_n^2/\beta_p^2 = R_f^T. \tag{5.4}$$

Moreover, as $|\rho_p| \ll 1$ because of the diffractive nature of the $\bar{p}$ interaction (see table 6), we assume also

$$|\rho_n| = |\rho_p| \ll 1\,. \tag{5.5}$$

Hence, considering eq. (5.4) and neglecting ρ_n and ρ_p, from eq. (5.1) we obtain

$$R_f^{el} = \sigma^{el}(\bar{p}n)/\sigma^{el}(\bar{p}p) = R_f^T \tag{5.6}$$

and, finally, as $\sigma = \sigma^a + \sigma^{el}$,

$$R_f^a = \sigma^a(\bar{p}n)/\sigma^a(\bar{p}p) = R_f^T = R_f^{el}\,. \tag{5.7}$$

In this way only R_f^T is a free parameter and we can fit our $\bar{p}^4$He total reaction cross section experimental values by the equation

$$\sigma_R = (4\pi/k)\ \mathrm{Im}\ F(0) - \int |F|^2\, d\Omega\,, \tag{5.8}$$

where $F(\Delta)$ is given by eq. (5.2).

As it concens the validity of the above assumptions, we observe that (i) values of $|\rho_p|$ and $|\rho_n| < 0.5$ have practically no influence on the total cross sections; (ii) a 20% change in the relation (5.4) only causes a 2–3% change in the value of σ_R; (iii) in ref. [6]) it is shown that for the $\bar{p}^2$H case between 300 and 600 MeV/c the values of R^T and R^{el} differ 15% on average (including experimental uncertainties of ~5%).

Now we discuss the values of σ_p, β_p^2 and ρ_p obtained in recent $\bar{p}p$ scattering experiments. The world data up to 1984 ($k > 250$ MeV/c), which is summarized in ref. [32]), is in partial disagreement with those from a LEAR experiment [31]) ($181 < k < 590$ MeV/c). One finds that it is possible to fit with an overall interpolation formula the ρ_p values (k in GeV/c):

$$\rho_p = \rho_n = 1.33 - 10.34k + 22.78k^2 - 13.63k^3\,, \tag{5.9}$$

whereas the same thing is not true for σ_p and β_p^2. Hence, we adopt two sets of values for σ_p and β_p^2 and perform a grid procedure with R_f^T as a free parameter, minimizing the difference between our experimental values of σ_R and those calculated by means of eq. (5.8).

The results are reported in table 5 and in fig. 2, where the error associated to R_f^T defines the interval where the calculated σ_R reproduce the experimental value within one standard deviation. This procedure determines, at each momentum, two estimations of R_f^T which can be compared with the R_b^a values obtained in the preceding section. At 200 MeV/c there is a large discrepancy in the values of R_f^T, which reflects the uncertainty on the $\bar{p}p$ parameters, and the value of R_b^a falls between the two values of R_f^T. At 300 MeV/c one finds $R_f^T \sim R_b^a$ and at 600 MeV/c it seems that $R_f^T > R_b^a$, which might be an indication of nuclear binding effects.

6. Discussion

6.1. COMPARISON WITH $\bar{p}^2$H AND $\bar{p}$-NUCLEUS RESULTS

The R_b^a values we have found are reported in fig. 4 together with R_b^a values obtained from $\bar{p}^2$H annihilation data following a similar procedure and with R_f^T values obtained from some analyses of experimental data performed in the frame of the Glauber theory. The latter ones concern both $\bar{p}^2$H [refs. [5,6,10])] and $\bar{p}$-nucleus data with mass number A ranging from 4 to 63 [refs. [1,9,12])]. We recall that, due to eq. (5.7), which is a usual approximation in Glauber theory analyses, comparing R_b^a with R_f^T is equivalent to comparing R_b^a with R_f^a.

The theoretical values obtained for the $\bar{p}^2$H interaction show two distinct types of behaviour depending on the different sets of experimental data analyzed. The black points and the dashed line on the figure were obtained from the total $\bar{p}^2$H

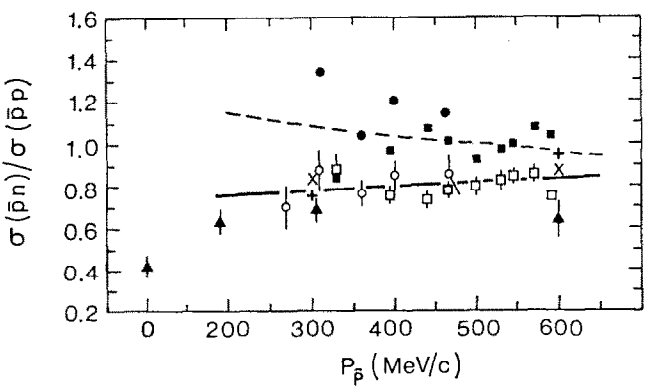

Fig. 4. Ratio between the $\bar{p}n$ and the $\bar{p}p$ cross sections versus $\bar{p}$ momentum. R_b^a values: (□) from $\bar{p}^2$H annihilation data of ref. [3]); (○) from $\bar{p}^2$H annihilation data of ref. [4]); (▲) from $\bar{p}^4$He data (this work). R_f^T values from Glauber theory analyses; (■) ref. [5]) concerning $\bar{p}^2$H total cross sections of ref. [3]); (●) ref. [7]) concerning $\bar{p}^2$H total cross sections of ref. [4]); (×) refs. [8,12]) with regard to $\bar{p}$-nucleus elastic scattering data; (+) from ref. [1]) with regard to $\bar{p}$-nucleus reaction cross-section data; broken line: analysis of the $\bar{p}^2$H total cross sections of ref. [4]); full line: analysis of $\bar{p}^2$H total cross section of ref. [10]). (Both lines from ref. [9]).)

cross-section values reported in refs. [3,4]) and the open points were obtained from the total cross-section values of ref. [10]). The latter cross-section values are systematically lower than the former ones (see fig. 5a) and the difference is due to lower total elastic cross-section values (see fig. 5c), while the annihilation cross-section values agree with each other (see fig. 5b). Also, the elastic cross-section values of ref. [4]) show an unexpected decrease at the lower momenta. We note that there is a substantial agreement between the R_f^T values obtained through the Glauber theory analysis of the ^{2}H data of ref. [10]) and the R_b^a values of refs. [3,4]).

For the annihilation of $\bar{p}$ at rest, ref. [4]) gives $R_b^a = 0.749 \pm 0.018$ and ref. [3]) 0.815 ± 0.0034, but in the first experiment at rest means a $\bar{p}$ momentum less than 260 MeV/c and in the latter one a $\bar{p}$ momentum less than about 300 MeV/c. Summarizing, the R_b^a values are on average 0.8 with a small decrease from 600 MeV/c down to rest.

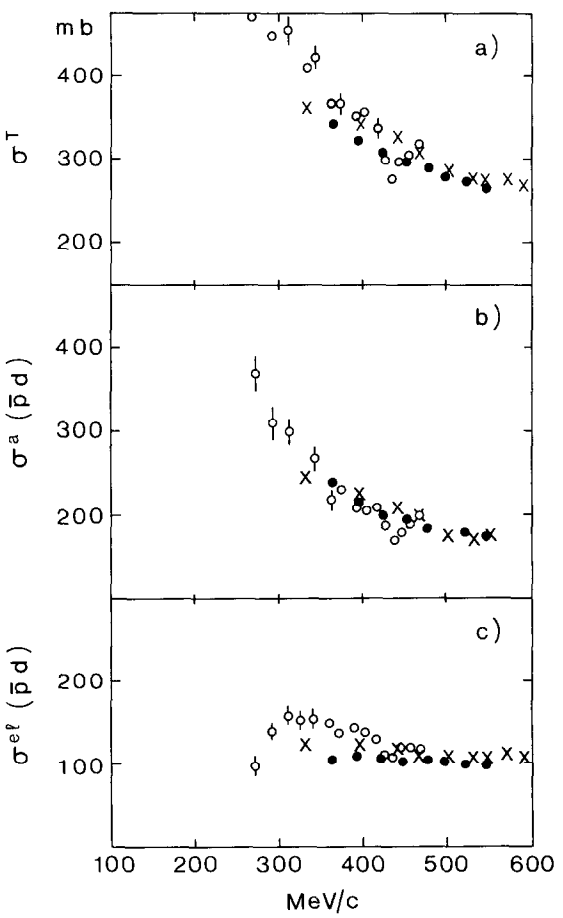

Fig 5. Total, annihilation and elastic $\bar{p}^2$H cross sections versus $\bar{p}$ momentum. Comparison among the data of ref. [3]) (×), ref. [4]) (○) and ref. [10]) (●).

Our R_b^a values are a little smaller than those obtained for ^{2}H between 300 and 600 MeV/c and decrease more and more as the $\bar{p}$ momentum goes down to zero (here, zero energy means $\bar{p}$ captured on atomic orbits). At 300 MeV/c the R_b^a value is equal to the R_f^T value obtained by the Glauber theory calculation. At 200 MeV/c the R_b^a value falls between the two calculated R_f^T values and at 600 MeV/c is a little smaller than the calculated R_f^T value.

Finally, we notice that very preliminary results [33]) from an experiment on anti-neutron–proton annihilation in the momentum range between 100 and 500 MeV/c show that $\sigma^a(\bar{n}p)$ is about $\frac{2}{3}\sigma^a(\bar{p}p)$, i.e. $R_f^T \approx 0.66$.

As a final remark, we recall also that values of R_f^T smaller than 1 are predicted by antinucleon–nucleon potential model calculations [34]) independently from the different forms assumed for the potentials.

7. Conclusions

Our main results are summarized in tables 4, 5 and 6 and fig. 2. They agree with $\bar{p}^2$H annihilation data and some Glauber theory analyses of $\bar{p}^2$H and $\bar{p}$-nucleus total cross sections and show that, within experimental uncertainty,

$$R_b^a \approx R_f^T < 1$$

with R increasing with the $\bar{p}$ momentum. Values of R_b^a smaller than 1 are supported also by preliminary results of an experiment on $\bar{n}p$ interaction [33]).

Our Glauber theory analysis of the $\bar{p}^4$He reaction cross section puts in evidence some discrepancies between experimental $\bar{p}p$ data at low energy [31,32]). Similarly, a comparison of some Glauber theory calculations of R_f^T performed by using different sets of $\bar{p}^2$H total cross sections shows some discrepancies among these experimental data [3,4,10]).

Thanks are due to Dr L.A. Kontratyuk and Dr M.G. Sapozhnikov, who discussed with us many aspects of our work and, very kindly, informed us in advance of some results of their analyses.

References

1) F. Balestra *et al.*, Nucl. Phys. **A452** (1986) 573
2) D. Garreta *et al.*, Phys. Lett. **135B** (1984) 266; **139B** (1984) 464; **169B** (1986) 14
3) R. Bizzarri *et al.*, Nuovo Cim. **22A** (1974) 225
4) T. Kalogeropoulos, G.S. Tzanakos, Phys. Rev. **D22** (1980) 2585
5) L.A. Kondratyuk, Sov. J. Nucl. Phys. **24** (1976) 247
6) L.A. Kontratyuk *et al.*, Sov. J. Nucl. Phys. **33** (1981) 413
7) L.A. Kondratyuk and M.Zh. Shmatikov, Phys. Lett. **117B** (1982) 38
8) O.D. Dalkarov and V.A. Karmanov, Nucl. Phys. **A445** (1985) 579 and Report n. 87, Lebedev Physical Institute, Moscow (1986)
9) L.A. Kondratyuk and M.G. Sapozhnikov, Yad. Fiz., submitted

10) R.P. Hamilton *et al.*, Phys. Rev. Lett. **44** (1980) 1182
11) K. Nakamura *et al.*, Phys. Rev. Lett. **52** (1984) 731
12) O.D. Dalkarov and V.A. Karmanov, Phys. Lett. **147B** (1984) 1
13) F. Balestra *et al.*, Phys. Lett. **165B** (1985) 265
14) F. Balestra *et al.*, CERN-EP/86-163 and Nucl. Instr. Meth. (in press)
15) F. Balestra *et al.*, Nucl. Instr. Meth. **A234** (1985) 30
16) U. Amaldi *et al.*, Nuovo Cim. **46A** (1966) 171
17) R. Armenteros and B. French, High-energy Physics, ed. E.H.S. Burhop (Academic Press, 1969) vol. 4, p. 237
18) R.P. Hamilton *et al.*, Phys. Rev. Lett. **44** (1980) 1179
19) K. Nakamura *et al.*, Phys. Rev. Lett. **53** (1984) 885
20) W. Brückner *et al.*, CERN-EP/85-202
21) V. Flaminio *et al.*, Report CERN-HERA/84-01, Geneva (1984)
22) T. Tsuboyama *et al.*, Phys. Rev. **D28** (1983) 2135
23) K. Nakamura *et al.*, Phys. Rev. **C31** (1985) 1853
24) D.R. Harrington, Phys. Rev. **184** (1969) 1745;
V.M. Eisenberg, Ann. of Phys. **71** (1972) 542;
S.J. Wallace, Adv. Nucl. Phys. **12** (1981) 135
25) V.B. Mandelzweig and S.J. Wallace, Phys. Rev. **C25** (1982) 61
26) V.M. Kolybasov and L.A. Kontratyuk, Phys. Lett. **39B** (1972) 439
27) R. Glauber and G. Matthiae, Nucl. Phys. **B21** (1970) 135
28) G.D. Alkhazov, S.L. Belostotsky and A.A. Vorobyov, Phys. Reports **42** (1978) 89
29) L.R.B. Elton, Nuclear sizes (Oxford University Press, 1961)
30) R.H. Bassel and C. Wilkin, Phys. Rev. **174** (1968) 1179
31) W. Brückner *et al.*, Phys. Lett. **166B** (1986) 113; **158B** (1985) 180
32) H. Iwasaki *et al.*, Nucl. Phys. **A433** (1985) 580
33) D.L. Lowenstein *et al.*, VII Symp. Antiproton interaction, Durham 1984, Inst. Phys. Conf. Ser. N. 73, sect. 5, p. 323;
L.S. Pinsky, Physics with antiprotons at LEAR in the ACOL era. Third Lear Workshop, Tignes (1985), p. 275
34) R.A. Bryan and R.J. Phillips, Nucl. Phys. **B5** (1968) 201;
T. Ueda, Progr. Theor. Phys. 62 (1979) 1670;
J.M. Richard and M.E. Sainio, Phys. Lett. **B110** (1980) 349